

# RANKL-binding peptide promotes ectopic bone formation induced by BMP-2 gene transfer in murine gastrocnemius muscle

Shigeki Nagahiro<sup>1</sup>, Tomoki Uehara<sup>1</sup>, Mariko Yamamoto Kawai<sup>2</sup>, Preksa Keo<sup>3</sup>, Toshimi Sato<sup>4</sup>, Hiroki Ochi<sup>5</sup>, Shingo Sato<sup>6</sup>, Shinji Kuroda<sup>7</sup>, Takashi Ono<sup>3</sup>, Michiyo Miyashin<sup>1</sup> and Kazuhiro Aoki<sup>8\*</sup>

<sup>1</sup>Department of Pediatric Dentistry / Dentistry for Persons with Special Needs, Graduate School of Medical and Dental Sciences, Tokyo Medical and Dental University, Tokyo, Japan

<sup>2</sup>Department of Medical Secretarial Arts, Kansai Women's College, Osaka, Japan

<sup>3</sup>Department of Orthodontic Science, Graduate School of Medical and Dental Sciences, Tokyo Medical and Dental University, Tokyo, Japan

<sup>4</sup>Department of Bio-Matrix (Pharmacology), Graduate School of Medical and Dental Sciences, Tokyo Medical and Dental University, Tokyo, Japan

<sup>5</sup>Department of Orthopaedic and Trauma Research, Graduate School of Medical and Dental Sciences, Tokyo Medical and Dental University, Tokyo, Japan

<sup>6</sup>Center for Innovative Cancer Treatment, Tokyo Medical and Dental University Hospital, Tokyo, Japan

<sup>7</sup>Department of Oral Implantology and Regenerative Dental Medicine, Graduate School of Medical and Dental Sciences, Tokyo Medical and Dental University, Tokyo, Japan

<sup>8</sup>Department of Basic Oral Health Engineering, Graduate School of Medical and Dental Sciences, Tokyo Medical and Dental University, Tokyo, Japan

## Abstract

Bone morphogenetic protein-2 (BMP-2) gene delivery is expected to be useful as a way to overcome protein delivery problems, such as the need for a scaffold and high dose of BMP-2 protein, and using non-viral vectors is known to be a safer gene delivery system than that using viral vectors for clinical application. However, the efficiency of the BMP-2 expression is very low when non-viral vectors are used. In the present study, we clarified the feasibility of RANKL-binding peptide, which has recently been recognized as a bone anabolic reagent, in bone formation induced by BMP-2 gene transfer using non-viral vectors. We induced ectopic bone in the gastrocnemius muscle of C57BL/6 mice by a single injection of GFP/BMP-2-expressing vector. Subcutaneous administration of RANKL-binding peptide increased the ectopic bone mass on days 14 and 21 after plasmid injection, and histological analyses showed the stimulation of bone formation activity of the ectopic bone compared to the vehicle-treated control. Micro computed tomography images showed that RANKL-binding peptide improved the microstructure of ectopic bone. Our results suggest that RANKL-binding peptide may be effective in promoting bone formation induced by BMP-2 gene transfer using non-viral vectors.

## Introduction

Bone morphogenetic protein-2 (BMP-2), a bone-formation inducer, has been widely used in bone regeneration [1]. However, there are several critical problems associated with its clinical application, such as the need for a scaffold material and a high dose to induce bone formation [2,3]. BMP-2 gene delivery is believed to be one way of overcoming these problems with protein delivery [1,2,4]. The direct injection of genetic materials, such as *via* a plasmid vector, can be performed to induce bone formation without using a scaffold material, since gene-transfected cells can release the protein similarly to the scaffold materials, releasing the protein sustainably over a given duration [2]. Gene transfer is therefore considered a promising approach to BMP-2 therapy.

Various routes for BMP-2 gene transfer have been developed, with two kinds of vectors mainly used: non-viral and viral vectors [1]. Since viral vectors have a higher gene transfer efficiency than non-viral vectors, bone induction is greater when the BMP-2 gene is transfected using a viral vector [5,6]. Indeed, when we used a non-viral vector of BMP-2 to induce bone through electroporation, very little ectopic bone

was generated in rat skeletal muscle [7,8]. Even after increasing the amount of plasmid used or the number of rounds of electroporation, the amount of bone induced was relatively unchanged [7]. Despite the development of a number of other methods for increasing the amount of bone induced using non-viral vectors, such as sonoporation (cell sonication) [9] and cationic polymers [1,10], the amount of bone induced remains insufficient for clinical applications.

The receptor activator of NF- $\kappa$ B ligand (RANKL)-binding peptide is known to accelerate BMP-2-induced bone formation both *in vitro*

**\*Correspondence to:** Kazuhiro Aoki, Professor, Department of Basic Oral Health Engineering, Graduate School of Medical and Dental Sciences, Tokyo Medical and Dental University, 1-5-45, Yushima, Bunkyo-ku, Tokyo, 113-8549, Japan, Tel: +81-3-5803-4641, E-mail: kazu.hpha@tmd.ac.jp

**Key words:** BMP-2, gene transfer, non-viral vector, RANKL-binding peptide, ectopic bone

**Received:** December 08, 2019; **Accepted:** December 30, 2019; **Published:** January 07, 2020

and *in vivo* [11-14]. RANKL-binding peptides are thought to bind to the cellular surface acceptor RANKL on osteoblasts, leading to the expression of Runx-2, a master gene of osteoblast differentiation [15,16]. While this strategy combining RANKL-binding peptide and BMP-2 in protein form has been shown to stimulate BMP-2-induced bone formation in many animal models [12-14,17], the stimulatory effects of RANKL-binding peptide on bone formation induced by BMP-2 gene transfer have not been investigated. Since the amount of bone induced by BMP-2 gene transfer was slight even when using electroporation as described above, we hypothesized that RANKL-binding peptide might stimulate the bone formation induced by a non-viral vector.

The present study therefore assessed the feasibility of RANKL-binding peptide in bone formation induced by BMP-2 gene transfer through electroporation using a non-viral vector.

## Materials and methods

### Plasmid DNA of BMP-2 and a RANKL-binding peptide

pEGFP-N1 plasmid vector (Clontech, Mountain View, CA, USA) harboring cDNA of human BMP-2 in the BamHI restriction enzyme region at the multicloning site was used for BMP-2 gene transfer [18]. WP9QY (W9; YCWSQYLCY), a RANKL-binding peptide [19], was kindly provided by JITSUBO Co., Ltd. (Kanagawa, Japan).

### Cell culture and gene transfer *in vitro*

ST2 cells (a murine osteoblastic cell line; RIKEN, Ibaragi, Japan) were seeded at  $1 \times 10^4$ /well in a 48-well plate and cultured in growth medium (DMEM) supplemented with 10% fetal bovine serum (FBS; GE Healthcare Japan, Tokyo, Japan) 1 day before lipofection. The next day, 0.2  $\mu\text{g}/\mu\text{L}$  of EGFP-hBMP-2 vector was diluted in Opti-MEM (Invitrogen, Carlsbad, CA, USA) and then mixed with Lipofectamine 2000 (Invitrogen) for lipofection. Twelve hours after lipofection, the medium was changed. One day after lipofection, the culture was stimulated with 100  $\mu\text{M}$  of W9. To the wells without W9, only vehicle was added. Ten days after lipofection, the cells were rinsed with phosphate-buffered saline (PBS), harvested, and lysed with lysis buffer (0.1% Triton-X; Nacalai Tesque Inc., Kyoto, Japan) including 10 mM Tris-HCL. The protein concentration in the lysis buffer was determined using a BCA Protein Assay Kit (Takara Bio Inc., Shiga, Japan), and the alkaline phosphatase (ALP) activity was measured using a Lab Assay ALP (Wako Pure Chemical Corp., Osaka, Japan) following the manufacturer's protocol and a microplate reader (iMark; Bio-Rad, Hercules, CA, USA).

### BMP-2 gene transfer in the gastrocnemius muscle *in vivo*

Eight-week-old male C57BL/6 mice were obtained from Nippon CLEA (Tokyo, Japan), and maintained as described elsewhere [20]. All animal experiments were approved by the Institutional Animal Care and Use Committee of Tokyo Medical and Dental University (Tokyo, Japan; authorization numbers: A2018-104C, A2019-155A). Before treatment, mice were anesthetized as previously described [21]. We performed BMP-2 gene transfer into mouse gastrocnemius muscle using the plasmid vector expressing BMP-2 via electroporation, as previously described [7,22,23] (Figure 1A).

### Quantification of GFP-BMP-2 fusion protein expressions in the gastrocnemius muscle

Eighteen mice were divided into 6 groups ( $n=3$ ) to clarify the amount of protein expression induced by *in vivo* gene transfer of the GFP-BMP-2 expression vector. Gene transfer to the gastrocnemius

muscle was performed as described above. Empty vector without the BMP-2 gene (pCAGGS) was injected as a control vector (mock). Mice were sacrificed under anesthesia by cervical dislocation on days 1, 7, or 14 after gene transfer (Figure 1B), and the gastrocnemius muscle was dissected. GFP fluorescence images at the gene transfer site were obtained by fluorescent microscopy (FSX100; Olympus, Tokyo, Japan) using the undecalcified sections prepared as previously described [13]. The dissected gastrocnemius muscle (0.15 g) was homogenized with 0.25 M sucrose by a Polytron homogenizer (type ABM; Nissei Inc., Osaka, Japan) and then centrifuged at 5,000 g for 10 min at 4 °C. The protein concentration in the supernatant was measured as described above. The GFP expression in the supernatant was measured using a GFP-specific ELISA kit (Cell Biolabs, Inc., San Diego, CA, USA), and the relative GFP protein expression (pg) against the total protein amount ( $\mu\text{g}$ ) was calculated. The total amount of BMP-2 was calculated from the GFP amounts.

### Experimental design of ectopic bone formation induced by BMP-2 gene transfer using RANKL-binding peptide

Ten mice were divided into 2 groups ( $n=5$ ), and *in vivo* gene transfer to the gastrocnemius muscle was performed as described above. After gene transfer, RANKL-binding peptide (W9; 10 mg/kg/day) or vehicle was subcutaneously administered using osmotic minipumps (Model 2001; Alzet, Palo Alto, CA, USA) to the BMP-2+W9 and BMP-2+VEH groups, respectively [24]. Alizarin complexone (20 mg/kg; Dojindo, Kumamoto, Japan) was injected on day 12 to measure the bone formation activity. The mice were sacrificed under anesthesia by cervical dislocation on day 21 (Figure 1C).

### Radiological assessments

Soft X-ray images were taken with a cabinet X-ray device (type SRO-M50; Sofron, Tokyo, Japan). *In vivo* microfocal computed tomography (R\_mCT2; Rigaku, Tokyo, Japan) was performed at

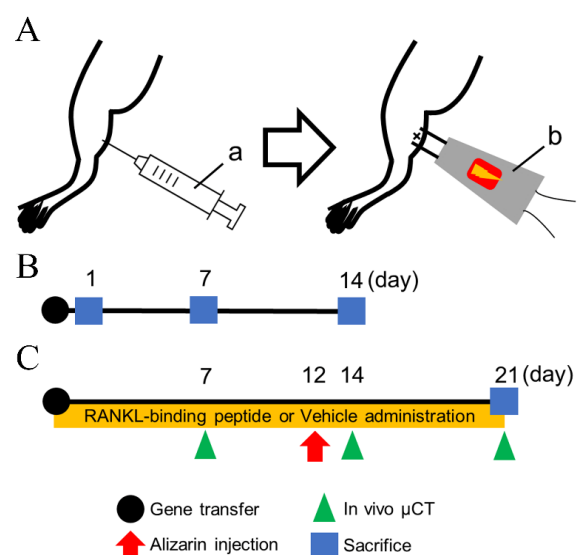


**Figure 1. Experimental design.** A. A schematic view of the gene transfer. Electroporation (100 V, 50 ms, 8 pulse) was carried out immediately after the injection of BMP-2-expressing plasmid vector (0.5  $\mu\text{g}/\mu\text{L}$ , total volume of 25  $\mu\text{L}$ ). (a) A 30-G syringe for plasmid injection. (b) Electroporator with needle-type electrodes. B. The GFP-BMP-2 expression was evaluated on days 1, 7, and 14. C. Osmotic minipumps filled with RANKL-binding peptide W9 or vehicle were subcutaneously implanted after gene transfer. *In vivo*  $\mu\text{CT}$  was performed weekly. Alizarin complexone for measuring the osteogenic activity was injected on day 12. Mice were sacrificed on day 21

90 kV, 160  $\mu$ A, and FOV 20 to obtain 3-dimensional bone images of each mouse every week until day 21. Micro-architectural changes in ectopic bone were measured using an image analysis software program (TRI/3D-BON; RATOC System Engineering, Tokyo, Japan) [25]. The reduction rate (%) was calculated as the ratio of the bone volume (BV) or bone surface (BS) on day 21 to that at day 14: [(BV or BS on day 14 – BV or BS on day 21) / (BV or BS on day 14)]  $\times$  100.

### Histological assessments and bone histomorphometry

We prepared undecalcified sections as previously described [13]. Some sections were stained with tartrate-resistant acid phosphatase (TRAP) or von Kossa for histological assessments. Bone resorption parameters (N.Oc/BS, Oc.S/BS) and the calcified tissue thickness in the ectopic bone were measured according to standard bone histomorphometric analyses [26]. Alizarin-labeled images were used to evaluate the bone formation activity in the ectopic bone. The same threshold value of fluorescent intensity on day 12 was used to analyze the alizarin-positive area in all samples, and the image was binarized for the area measurement using the ImageJ software program (version 1.50i; NIH, Bethesda, MD, USA).

### Statistical analyses

All data are presented as the means  $\pm$  standard deviation (SD). The statistical significance between two groups was compared using an unpaired *t*-test. Multiple groups comparisons were performed using a one-way analysis of variance and Tukey's multi-comparison *post hoc* test. *P* values of  $<0.05$  were considered to be significant. We also assumed that  $0.05 < P < 0.1$  indicated edge cases of significance or were highly suggestive of significance, according to the statement by the American Statistical Association [27,28].

## Results

### Effects of RANKL-binding peptide W9 on osteoblast differentiation in BMP-2-gene-transfected ST2 cells

To investigate whether or not W9 exerts a synergistic effect on osteoblast differentiation in BMP-2-gene transfected cells *in vitro*, we first added 100  $\mu$ M of W9 to ST2-cell culture. As shown in Figure 2A, 100  $\mu$ M of W9 stimulated the activity of ALP, a marker of early osteoblast differentiation, without BMP-2 gene transfection. Although no significant increase in ALP activity was noted in the BMP-2-gene-transfected wells compared to the vehicle control (0  $\mu$ M W9), an increase was observed in the presence of 100  $\mu$ M of W9 in the BMP-2-gene-transfected ST2 cells. Furthermore, it was also detected when

compared to the culture with 100  $\mu$ M of W9 in ST2 cells without BMP-2 gene transfer.

### Chronological changes in GFP-BMP-2 fusion protein expression after gene transfer in gastrocnemius muscle

We measured the GFP protein expression on days 1, 7, and 14 after gene transfer in the gastrocnemius muscle to evaluate the chronological changes in the GFP-BMP-2 fusion protein expression. As shown in Figure 2B, GFP-fluorescent-positive cells at the injection site of the plasmid vector were detected in the histological sections of the gastrocnemius muscle on day 1 after gene transfer, and these cells were increased on day 7 and were still observed on day 14 after gene transfer. The fluorescent images from the specimens after the transfection of the empty vector did not show any GFP-positive cells at any time points (Figure 2B). Quantitative analyses of the relative GFP expression confirmed these observations (Figure 2C). When we calculated the total amount of BMP-2 protein in the whole sample dissected from the gastrocnemius muscle, the average amount was 53, 129, and 100 pg on days 1, 7, and 14, respectively (Table 1).

### Effects of W9 on the microstructure of ectopic bone induced by BMP-2 gene transfer

To investigate the effects of W9 on the bone mass and microstructure of the ectopic bone induced by BMP-2 gene transfer, W9 or vehicle was subcutaneously administered to BMP-2-gene-transfected mice. Radiological images showed a greater amount of ectopic bone in the BMP-2+W9 group than in the BMP-2+VEH group (Figures 3A and B), and the bone volume analyses, such as the BMD and BV/TV, of the ectopic bone confirmed these observations (Figures 3C and D). The SMI, an indicator of a plate-like structure, was significantly lower in the BMP-2+W9 group than in the BMP-2+VEH group on day 14, and all parameters related to the bone microstructure were significantly changed on day 21, showing improvement in the bone microstructure (Figures 3E-3H). The reduction rate of the ectopic bone from day 14 to day 21 was slower in the BMP-2+W9 group than in the BMP-2+VEH group (Figures 3I and 3J).

### Effects of W9 on osteoclast formation and bone formation activity of ectopic bone induced by BMP-2 gene transfer

To clarify the functional role of W9 on BMP-2-gene-transfer-induced bone, histological analyses were performed. As shown in

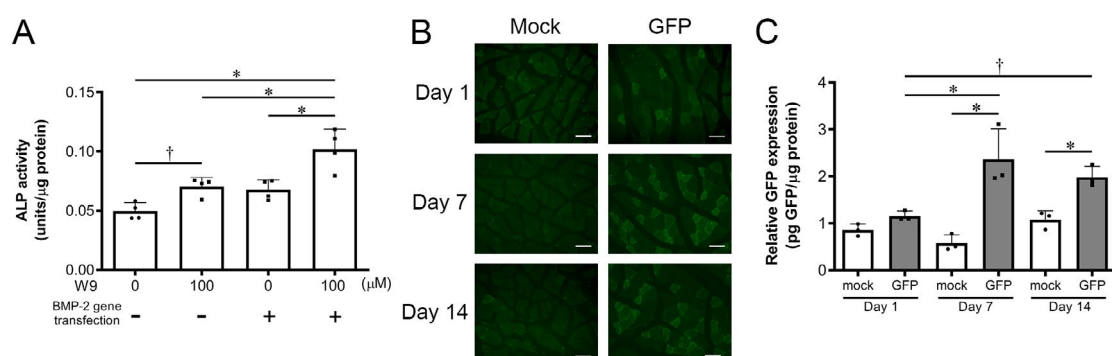
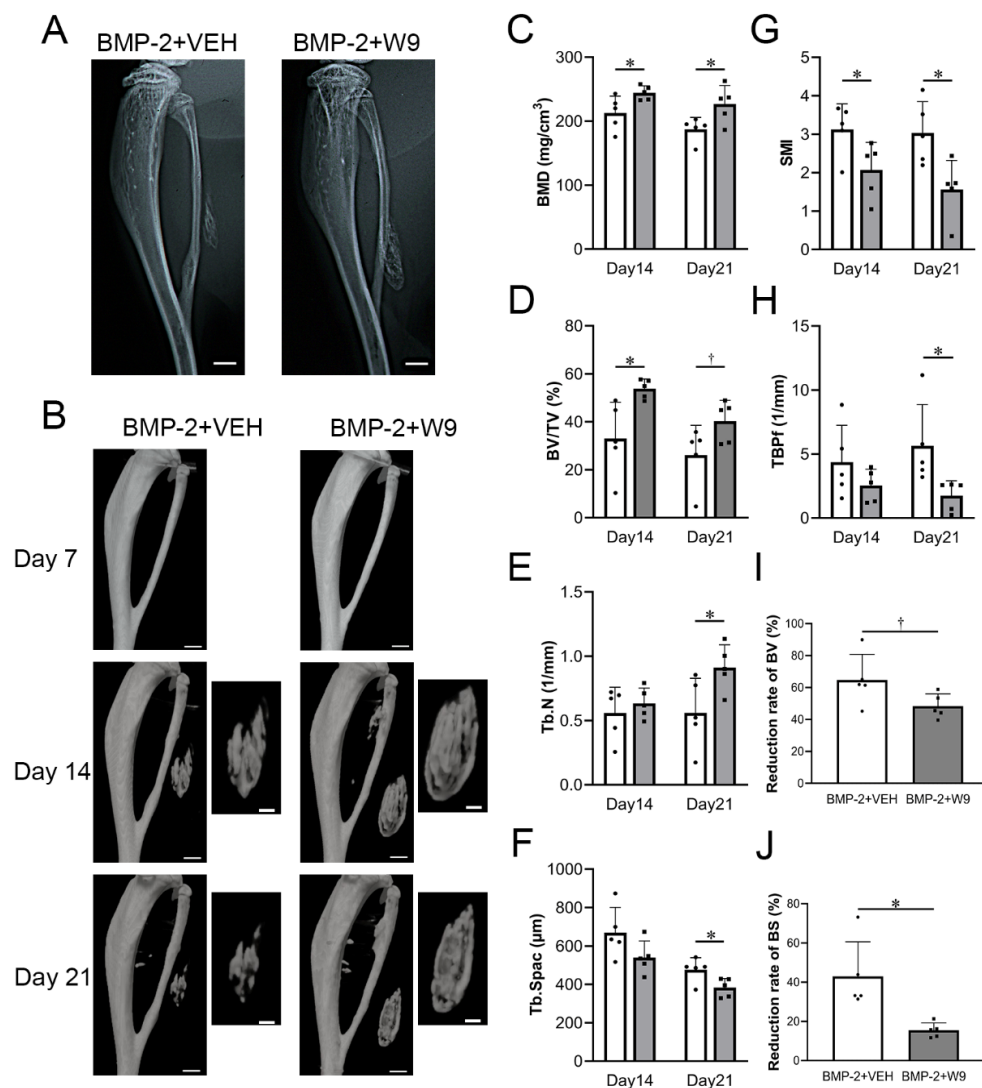


**Figure 2. W9 promoted osteoblast differentiation in ST2 cells *in vitro* and chronological changes in the GFP-BMP-2 fusion protein expression *in vivo*.** A. ALP activity in ST2 cells with or without transfection of a BMP-2 gene-expressing plasmid vector in the presence or absence of 100  $\mu$ M W9 on day 10 after gene transfection. Data are shown as the mean  $\pm$  SD. \* $p < 0.05$ .  $^{\dagger}0.05 < p < 0.1$ . B. Fluorescence images of GFP-positive muscle cells on days 1, 7, and 14 after GFP-BMP2 gene transfer (GFP) or empty vector transfer (mock). Scale bars=0.05 mm. C. Relative GFP expression on days 1, 7, and 14 after gene transfer. Data are shown as the mean  $\pm$  SD. \* $p < 0.05$ .  $^{\dagger}0.05 < p < 0.1$

**Table 1.** The amount of protein in the GFP-BMP-2-gene transfected gastrocnemius muscle

|                           | Day 1    | Day 7      | Day 14     |
|---------------------------|----------|------------|------------|
| GFP (pg)                  | 55.1±6.9 | 134.0±36.4 | 104.8±17.1 |
| BMP-2 (pg)                | 53.1±6.7 | 129.1±35.0 | 100.9±16.5 |
| Total protein amount (μg) | 47.5±2.4 | 56.1±3.6   | 52.5±3.8   |

The GFP concentration in the homogenized tissue solution from the dissected muscle, which was transfected by plasmid vector including the GFP-BMP-2 gene, were measured using an ELISA kit. Then, the GFP amount in the dissected muscle was calculated from the GFP concentration measured by ELISA. The total amount of BMP-2 was calculated from the GFP amounts. The total protein amount in the dissected muscle was measured using a standard protocol. The details have been described in the Materials and Method section. Data are shown as the mean ± SD (n=3)



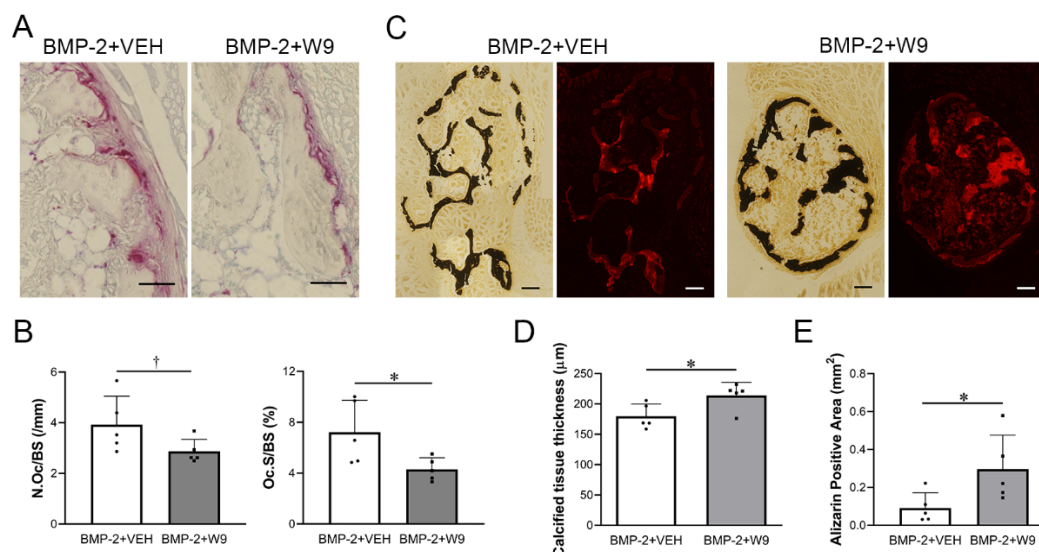
**Figure 3.** Radiological analyses revealed increased ectopic bone formation and structurally improved bone induced by BMP-2-gene transfer in the W9-treated group. A. Soft X-ray photographic images. BMP-2+VEH: BMP-2 gene transfer + vehicle-treated group, BMP-2+W9: BMP-2 gene transfer + W9-treated group. Scale bars=1 mm. B.  $\mu$ CT images of lower limb and ectopic bone on days 7, 14, and 21. Scale bars=1 mm (low magnification), 0.5 mm (high magnification). C. Bone mineral density (BMD) D. Ratio of bone volume (BV) to tissue volume (TV) E. Trabecular number (Tb.N) F. Trabecular spacing (Tb.Spac) G. Structure model index (SMI) H. Trabecular bone pattern factor (TBPF) I and J. The reduction rate calculated from the BV and BS on days 14 and 21. White bar: BMP-2+VEH, Gray bar: BMP-2+W9. Data are shown as the mean ± SD. \* $p < 0.05$  vs. Ctr. † $0.05 < p < 0.1$  vs. Ctr

Figure 4A, TRAP-positive cells were less frequent in the BMP-2+W9 group than in the BMP-2+VEH group. The alizarin-labeled area, which indicated the active bone formation area, seemed to be larger in the BMP-2+W9 group than in the BMP-2+VEH group. Quantitative analyses confirmed these observations (Figures 4B and E). The calcified tissue thickness also confirmed radiological observations of ectopic bone (Figures 3B and 4D).

## Discussion

The amount of BMP-2 protein needed to induce bone formation is far beyond the physiological amount that is available [2]. In our previous study,  $1 \times 10^6$  pg of BMP-2 was deemed necessary to form bone [29], and  $3 \times 10^5$  pg of BMP-2 was unable to form bone efficiently in a bone defect model [14]. In the present study, the amount of BMP-2





**Figure 4. W9 inhibited osteoclast formation and accelerated mineralization of ectopic bone induced by BMP-2 gene transfer.** A. TRAP-stained images of ectopic bone. TRAP-positive cells are shown in red. Scale bars=0.05 mm. B. Number of osteoclast/bone surface (N.Oc/BS), osteoclast surface/bone surface (Oc.S/BS). C. Bright field images of von-Kossa-stained undecalcified sections of ectopic bone (calcified tissue is shown in black). Fluorescent images of the alizarin-positive area (shown in red). Scale bars=0.1 mm. D. Calcified tissue thickness calculated based on the von-Kossa-positive area and perimeter. E. A quantitative analysis of the alizarin-positive area. Data are shown as the mean  $\pm$  SD. \* $p < 0.05$  vs. Ctr. † $0.05 < p < 0.1$  vs. Ctr. See Figure 3A for other definitions

protein expressed in the dissected gastrocnemius muscle at the BMP-2 gene transfer site was less than 200 pg at all time points after gene transfer during the experiments (Table 1). Since the amount of protein in the bone defect model was the total amount of BMP-2 incorporated in the scaffold material available for 28 days, while it was measured in the dissected gastrocnemius muscle at each time point in the present study, it might not be possible to compare these two studies. However, our findings suggest at least that very little BMP-2 was required to induce bone formation, although the amount formed was very small (Figure 3).

Since a high level of BMP-2 has been recognized as a cause of inflammation and/or carcinogenicity [30], many studies have attempted to reduce the amount of BMP-2 needed to induce bone formation. The BMP-2 expression in our study was very low, as shown in Table 1, suggesting that gene therapy using a BMP-2 plasmid vector may be a promising therapy; however, the actual bone formation induced by BMP-2 gene transfer alone was consequently quite little. In the present study, we used RANKL-binding peptide to increase the bone formation induced by BMP-2 gene transfer through electroporation, and this approach actually significantly enhanced the BV/TV and alizarin-positive area compared to the vehicle control group (Figures 3D and 4E), suggesting that RANKL-binding peptide stimulated BMP-2-gene-transfer-induced bone formation. We also found that RANKL-binding peptide increased the bone quality, as indicated by improvement in microstructural parameters such as the SMI and TBPf (Figures 3E-3H) [25]. The present study revealed the beneficial effects of RANKL-binding peptide on bone formation and the quality of bone induced by BMP-2 gene transfer.

Ectopic bone formation was not detected on day 7 and only first appeared from day 14 after gene transfer in both the vehicle and RANKL-binding peptide-treated groups (Figure 3B). The BV/TV was increased on day 14 (Figure 3D), and the alizarin-positive area, which was the indicator of bone formation activity, was increased on day 12 after gene transfer in the RANKL-binding peptide group compared to the vehicle control group (Figure 4E). These results suggest that

the increase in the bone formation activity on day 12 may lead to an increase in the ectopic bone volume induced by BMP-2 gene transfer.

## Conclusion

Our data suggest that RANKL-binding peptide was effective in promoting bone formation induced by BMP-2 gene transfer through electroporation using a non-viral vector. Therefore, the combination of the use of RANKL-binding peptide and the BMP-2 gene transfer might be an innovative method for use in bone regenerative therapy.

## Acknowledgements

The authors thank Drs. Yukihiro Tamura, Hitoyata Shimokawa, (Graduate School of Medical and Dental Sciences, Tokyo Medical and Dental University, Tokyo, Japan) for their support of this experiment.

## Funding

This study was supported by JSPS KAKENHI to TU (17K17314) and KA (17K11900).

## Conflicts of interest

The authors declare no conflicts of interest.

## References

- Park SY, Kim KH, Kim S, Lee YM, Seol YJ (2019) BMP-2 gene delivery-based bone regeneration in dentistry. *Pharmaceutics* 11(8).
- Fischer J, Kolk A, Wolfart S, Pautke C, Warnke PH, et al. (2011) Future of local bone regeneration - Protein versus gene therapy. *J Craniomaxillofac Surg* 39(1): 54-64.
- Sheikh Z, Javaid MA, Hamdan N, Hashmi R (2015) Bone regeneration using bone morphogenetic proteins and various biomaterial carriers. *Materials (Basel)* 8(4): 1778-1816.
- Im GI (2013) Nonviral gene transfer strategies to promote bone regeneration. *J Biomed Mater Res A* 101(10): 3009-18.
- Sugiyama O, An DS, Kung SP, Feeley BT, Gamradt S, et al. (2005) Lentivirus-mediated gene transfer induces long-term transgene expression of BMP-2 *in vitro* and new bone formation *in vivo*. *Mol Ther* 11(3): 390-398.

6. Abe N, Lee YP, Sato M, Zhang X, Wu J, et al. (2002) Enhancement of bone repair with a helper-dependent adenoviral transfer of bone morphogenetic protein-2. *Biochem Biophys Res Commun* 297(3): 523-527.
7. Kawai M, Bessho K, Kaihara S, Sonobe J, Oda K, et al. (2003) Ectopic bone formation by human bone morphogenetic protein-2 gene transfer to skeletal muscle using transcutaneous electroporation. *Hum Gene Ther* 14(16): 1547-1556.
8. Kawai M, Maruyama H, Bessho K, Yamamoto H, Miyazaki J, et al. (2009) Simple strategy for bone regeneration with a BMP-2/7 gene expression cassette vector. *Biochem Biophys Res Commun* 390(3): 1012-1017.
9. Osawa K, Okubo Y, Nakao K, Koyama N, Bessho K (2009) Osteoinduction by microbubble-enhanced transcutaneous sonoporation of human bone morphogenetic protein-2. *J Gene Med* 11(7): 633-641.
10. Komatsu K, Shibata T, Shimada A, Ideno H, Nakashima K, et al. (2016) Cationized gelatin hydrogels mixed with plasmid DNA induce stronger and more sustained gene expression than atelocollagen at calvarial bone defects *in vivo*. *Journal of Biomaterials Science-Polymer Edition* 27(5): 419-430.
11. Furuya Y, Inagaki A, Khan M, Mori K, Penninger JM, et al. (2013) Stimulation of bone formation in cortical bone of mice treated with a receptor activator of nuclear factor-kappaB ligand (RANKL)-binding peptide that possesses osteoclastogenesis inhibitory activity. *J Biol Chem* 288(8): 5562-5571.
12. Masud Khan AA, Alles N, Soysa NS, Al Mamun MA, Nagano K, et al. (2013) The local administration of TNF- $\alpha$  and RANKL antagonist peptide promotes BMP-2-induced bone formation. *Journal of Oral Biosciences* 55(1): 47-54.
13. Uehara T, Mise-Omata S, Matsui M, Tabata Y, Murali R, et al. (2016) Delivery of RANKL-Binding Peptide OP3-4 Promotes BMP-2-induced maxillary bone regeneration. *J Dent Res* 95(6): 665-672.
14. Sugamori Y, Mise-Omata S, Maeda C, Aoki S, Tabata Y, et al. (2016) Peptide drugs accelerate BMP-2-induced calvarial bone regeneration and stimulate osteoblast differentiation through mTORC1 signaling. *Bioessays* 38(8): 717-725.
15. Sone E, Noshiro D, Ikebuchi Y, Nakagawa M, Khan M, et al. (2019) The induction of RANKL molecule clustering could stimulate early osteoblast differentiation. *Biochemical and Biophysical Research Communications* 509(2): 435-440.
16. Ikebuchi Y, Aoki S, Honma M, Hayashi M, Sugamori Y, et al. (2018). Coupling of bone resorption and formation by RANKL reverse signalling. *Nature* 561(7722): 195-200.
17. Arai Y, Aoki K, Shimizu Y, Tabata Y, Ono T, et al. (2016) Peptide-induced de novo bone formation after tooth extraction prevents alveolar bone loss in a murine tooth extraction model. *Eur J Pharmacol* 782: 89-97.
18. Oda M, Kuroda S, Kondo H, Kasugai S (2009) Hydroxyapatite fiber material with BMP-2 gene induces ectopic bone formation. *J Biomed Mater Res B Appl Biomater* 90(1): 101-109.
19. Aoki K, Saito H, Itzstein C, Ishiguro M, Shibata T, et al. (2006) A TNF receptor loop peptide mimic blocks RANKL ligand-induced signaling, bone resorption, and bone loss. *J Clin Invest* 116(6): 1525-1534.
20. Saito H, Kojima T, Takahashi M, Horne WC, Baron R, et al. (2007) A tumor necrosis factor receptor loop peptide mimic inhibits bone destruction to the same extent as anti-tumor necrosis factor monoclonal antibody in murine collagen-induced arthritis. *Arthritis and Rheumatism* 56(4): 1164-1174.
21. Haque Bhuyan MZ, Tamura Y, Sone E, Yoshinari Y, Maeda C, et al. (2017) The intra-articular injection of RANKL-binding peptides inhibits cartilage degeneration in a murine model of osteoarthritis. *J Pharmacol Sci* 134(2): 124-130.
22. Kawai M, Kataoka YH, Sonobe J, Yamamoto H, Inubushi M, et al. (2018) Non-surgical model for alveolar bone regeneration by bone morphogenetic protein-2/7 gene therapy. *J Periodontol* 89(1): 85-92.
23. Yamamoto H, Kawai M, Shiotsu N, Watanabe M, Yoshida Y, et al. (2012) BMP-2 gene transfer under various conditions with *in vivo* electroporation and bone induction. *Journal of Oral and Maxillofacial Surgery, Medicine, and Pathology* 24(1): 49-53.
24. Kato G, Shimizu Y, Arai Y, Suzuki N, Sugamori Y, et al. (2015) The inhibitory effects of a RANKL-binding peptide on articular and periarticular bone loss in a murine model of collagen-induced arthritis: a bone histomorphometric study. *Arthritis Res Ther* 17: 251.
25. Bouxsein ML, Boyd SK, Christiansen BA, Guldberg RE, Jepsen KJ, et al. (2010) Guidelines for assessment of bone microstructure in rodents using micro-computed tomography. *Journal of Bone and Mineral Research* 25(7): 1468-1486.
26. Dempster DW, Compston JE, Drezner MK, Glorieux FH, Kanis JA, et al. (2013) Standardized nomenclature, symbols, and units for bone histomorphometry: A 2012 update of the report of the ASBMR Histomorphometry Nomenclature Committee. *J Bone Miner Res* 28(1): 2-17.
27. Yaddanapudi LN (2016) The American Statistical Association statement on P-values explained. *J Anaesthesiol Clin Pharmacol* 32(4): 421-423.
28. Baker M (2016) Statisticians issue warning over misuse of P values. *Nature* 531(7593): 151.
29. Al Mamun MA, Khan MAAM, Alles N, Matsui M, Tabata Y, et al. (2013) Gelatin hydrogel carrier with the W9-peptide elicits synergistic effects on BMP-2-induced bone regeneration. *Journal of Oral Biosciences* 55(4): 217-223.
30. James AW, LaChaud G, Shen J, Asatrian G, Nguyen V, et al. (2016) A review of the clinical side effects of bone morphogenetic protein-2. *Tissue Eng Part B Rev* 22(4): 284-297.